

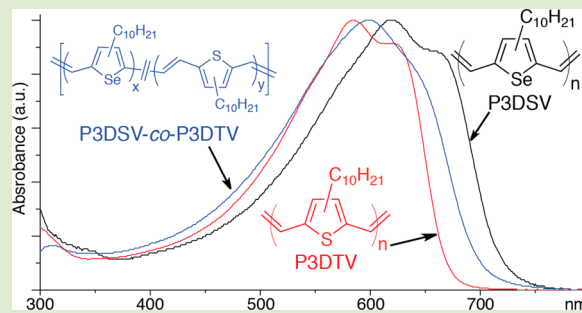
# Synthesis and Characterization of Poly(selenylene vinylene) and Poly(selenylene vinylene)-*co*-Poly(thienylene vinylene) through Acyclic Diene Metathesis (ADMET) Polymerization

Zhen Zhang and Yang Qin\*

Department of Chemistry and Chemical Biology, University of New Mexico, MSC03 2060, 1 UNM, Albuquerque, New Mexico 87131, United States

## Supporting Information

**ABSTRACT:** We report the synthesis and characterization of poly(3-decylselenylene vinylene) (P3DSV) homopolymers and poly(3-decylselenylene vinylene)-*co*-poly(3-decylthienylene vinylene) (P3DSV-*co*-P3DTV) copolymers through acyclic diene metathesis (ADMET) polymerization techniques. The obtained polymers were fully characterized. P3DSV was found to possess reduced crystallinity and a smaller bandgap of about 1.6 eV, compared with those of poly(3-decylthienylene vinylene) (P3DTV) analogs. P3DSV-*co*-P3DTV shows electronic properties between those of the corresponding homopolymers and distinctly different from those of simple blends of the two homopolymers. Our methodology provides a new way to control the physical and electronic properties



of low bandgap poly(arylene vinylene)s (PAVs).

Conjugated polymers (CPs) have found widespread applications in solution processed thin film electronic devices.<sup>1</sup> CPs possessing low electronic bandgaps are especially attractive in optoelectronic devices including organic photovoltaics (OPVs).<sup>2–4</sup> Among a plethora of examples, low bandgap poly(thienylene vinylene) (PTV) derivatives have attracted increasing attention due to high charge mobilities,<sup>5</sup> environmental and thermal stability,<sup>1</sup> and recently discovered singlet fission processes.<sup>6</sup> Various synthetic methods have been developed and refined over the years for PTV preparation, including earlier examples involving Gilch-type reactions and elimination from soluble polymeric precursors,<sup>7–9</sup> McMurry coupling, and Wittig-type reactions of aldehyde-containing monomers,<sup>10–12</sup> transition metal catalyzed cross-coupling reactions,<sup>13–15</sup> and, more recently, acyclic diene metathesis (ADMET) polymerization of thiophene monomers bearing double bonds at 2,5-positions.<sup>16–21</sup> Applications of these soluble PTVs have been attempted in OPV devices, but only low to moderate device efficiencies have been obtained.<sup>22–24</sup> Despite morphology controllability issues,<sup>25</sup> extremely short exciton lifetimes in PTVs due to ultrafast nonradiative decay rates have been ascribed as the main reasons for low OPV performances.<sup>6,26</sup> Thus, in order for PTVs to be more applicable for OPV and other optoelectronic devices, structural modifications and subsequent optimization in physical/electronic properties are necessary.

One such structural modification is to replace the sulfur atoms in PTVs with selenium, the next heavier element in group 16, generating poly(selenylene vinylene)s (PSVs). The larger sizes, enhanced polarizability, and stronger spin-orbit coupling effects of selenium atoms are expected to result in

significantly different physical/electronic properties over their sulfur counterparts.<sup>27–29</sup> For instance, poly(3-alkylselenophene)s (P3ASs) have been shown to possess smaller bandgaps and lower ionization potentials than that of the well-studied poly(3-alkylthiophene)s (P3ATs).<sup>30,31</sup> Heeney et al. and Zade et al. recently reported the preparation of alkyl- and cycloalkyl-substituted PSV derivatives, respectively, through palladium-catalyzed Stille coupling reactions.<sup>32,33</sup> During their synthesis, an AA + BB type condensation reaction was applied, which requires strict stoichiometry in order to achieve high molecular weights. ADMET, on the other hand, uses a single type of monomer, is compatible with a variety of functional groups, and provides versatile end-group controllability.<sup>34–36</sup> Preparation of PSV derivatives through ADMET has not been demonstrated.

Furthermore, by partially substituting the sulfur atoms in PTVs with selenium, copolymers of PTV and PSV are obtained, which provides additional pathways to further fine-tune the polymer properties. Such a strategy has been applied in the synthesis of copolymers of P3AS and P3AT, which displayed tunable physical and electronic properties.<sup>37</sup> To the best of our knowledge, there have been no examples of such copolymers involving both PTV and PSV structures.

Herein, we report the synthesis of poly(3-decylselenylene vinylene) (P3DSV) and its random copolymer with thienylene vinylene units, poly(3-decylselenylene vinylene)-*co*-poly(3-decylthienylene vinylene) (P3DSV-*co*-P3DTV), through

Received: May 1, 2015

Accepted: June 7, 2015

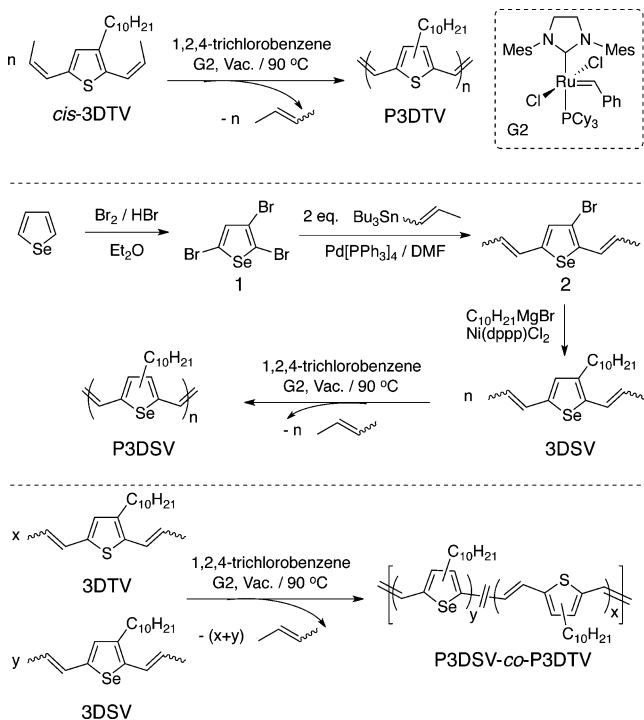
Published: June 10, 2015



ADMET polymerization techniques. P3DSV displays distinctly different properties from those of P3DTV, which can be further tuned through copolymerization.

The synthetic methods are summarized in Scheme 1 and detailed procedures are described in the Supporting Information (SI). Preparation of P3DTV ( $M_n = 21.3$  kDa,  $\bar{D} = 2.1$ , SEC) has been reported previously.<sup>21</sup>

### Scheme 1. Synthetic Methods



For the synthesis of the Se containing monomer, 3DSV, we started with selenophene. Tribromination using  $\text{Br}_2/\text{HBr}$  led smoothly to monomer **1** that has been fully characterized by  $^1\text{H}$  and  $^{13}\text{C}$  NMR spectroscopy as well as GC-MS analysis (Figure S1). Cross-coupling reaction of **1** with exactly two equivalents of *trans/cis* mixture of tri-*n*-butyl(1-propenyl)tin (mixture of *trans* and *cis* isomers) led to monomer **2**. The substitution took place only at the 2 and 5 positions of monomer **1** due to the enhanced reactivity, which was further proved after the next reaction step—alkylation at the 3 position through Grignard cross-coupling reaction leading to monomer 3DSV. GC-MS analysis of 3DSV proves the presence of several stereoisomers and possible regioisomers having exactly the same molecular weight for the expected structures (Figure S2).<sup>38</sup> The  $^1\text{H}$  NMR spectrum of 3DSV is very similar to those of related 2,5-dipropenylthiophene analogs<sup>17,21</sup> prepared from 3-alkylthiophene derivatives (Figure 1). Signals from the  $\text{CH}_2$  group attached to the selenophene ring appear at about 2.5 ppm that is typical of alkyl chains substituted at the 3-position, while chemical shifts from 2- or 5-substituted alkyl chains have been well-documented to appear at about 2.8–2.9 ppm.<sup>39</sup> The absence of any signals in the 2.8–2.9 ppm region confirms the substitution pattern in 3DSV and selectivity of the cross-coupling reaction leading to monomer **2**. Due to the unsymmetrical nature of 3DSV, there are four stereoisomers originated from combinations of *trans* and *cis* configurations of the 2- and 5-propenyl groups, respectively. From NMR integration, these isomers exist in roughly equal amount, which is not surprising since we started

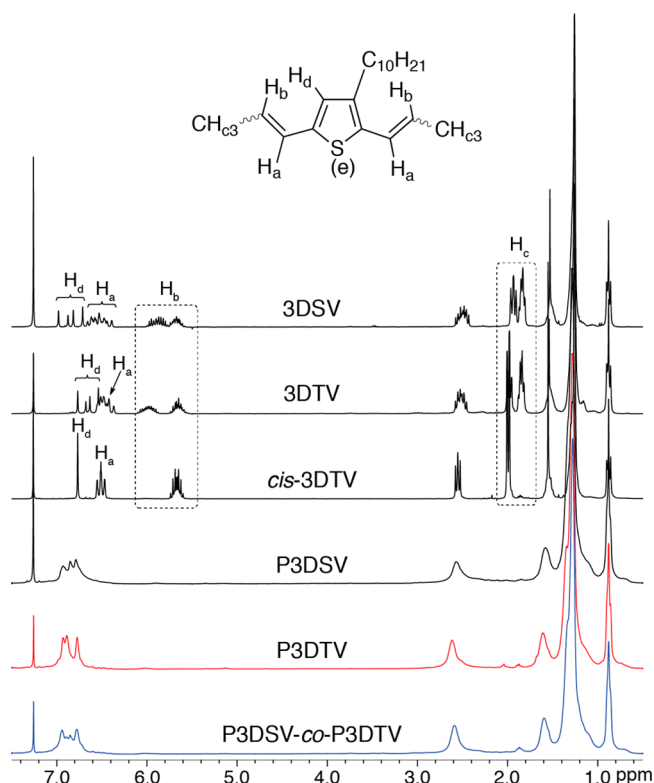


**Figure 1.**  $^1\text{H}$  NMR spectra overlay of 3DSV, 3DTV, *cis*-3DTV, P3DSV, P3DTV, and P3DSV-co-P3DTV.

with a *trans/cis* mixture of tri-*n*-butyl(1-propenyl)tin and the Stille coupling reaction applied has no stereoselectivity. It is worth noting that the thiophene monomer used for P3DTV synthesis, *cis*-3DTV, is a single stereoisomer having exclusively *cis* double bonds (Figure 1) and has displayed faster ADMET polymerization rates over corresponding stereoisomer mixtures. However, during the synthesis of *cis*-3DTV, excess of Grignard reagents were applied, which is less amenable for the synthesis of 3DSV. We are currently optimizing the reaction conditions and seeking alternative routes for the preparation of 3DSV containing exclusively *cis* double bonds.

ADMET polymerization of 3DSV was conducted in 1,2,4-trichlorobenzene (TCB) under dynamic vacuum at 90 °C using Grubbs second generation catalyst (G2, Scheme 1). Under such conditions, TCB was continuously refluxing, which could efficiently remove the 2-butene byproducts and drive the polymerization to high monomer conversions. The reaction mixture gradually turned from slightly yellow to red, then purple and eventually blue, indicating evolution of the conjugation lengths in P3DSV. The polymer was isolated by precipitation into methanol and purified by Soxhlet extraction as a black solid ( $M_n = 14.3$  kDa,  $\bar{D} = 1.8$ , SEC). The molecular weight is relatively smaller than that of P3DTV, presumably due to the presence of *trans* double bonds that have sluggish polymerization rates. The NMR spectra of P3DSV are very similar to those of P3DTV (Figure 1), in which signals are broad and no splitting patterns can be observed in the  $^1\text{H}$  spectrum. These observations are consistent with previous reports on PTVs obtained through ADMET and indicate regiorandom nature of the P3DSV structure, different from the regioregular polymers synthesized from Horner-Emmons and Stille coupling reactions.<sup>12,32</sup> In order to prepare the copolymer and to avoid large difference in monomer polymerization rates,

we prepared another 3DTV monomer having similar *trans/cis* ratios as those in 3DSV through Stille coupling reaction of 2,5-dibromo-3-decylthiophene with tri-*n*-butyl(1-propenyl)tin.<sup>21</sup> Kinetics studies of the initial polymerization periods show comparable polymerization rates for both 3DSV and 3DTV, which are significantly lower than that of *cis*-3DTV, as shown in Figure S3. We thus expect the copolymer to be more likely random in nature. P3DSV-*co*-P3DTV was thus synthesized starting with a mixture of these two monomers in equal molar ratio (3DSV/3DTV  $\sim$  10/9 by wt.) leading to a black solid ( $M_n$  = 8.1 kDa,  $D$  = 1.8, SEC). NMR spectra of the resulting P3DSV-*co*-P3DTV show broad overlapping signals with contributions from 3DSV and 3DTV units, confirming incorporation of both monomers (Figure 1).

The newly prepared polymers were first characterized by Raman and infrared (IR) spectroscopy (Figure S4). For better comparison, data for P3DTV and an equal weight blend of P3DSV and P3DTV are also included. All polymers and blends show very similar Raman scattering profiles (Figure S4A). The three major peaks between 1200 and 1600  $\text{cm}^{-1}$  have been previously assigned to vinyl C–H bend, ring C=C stretch and vinyl C=C stretch (from low to high Raman shifts).<sup>25</sup> Noticeably, the three peaks for P3DSV at 1277, 1394, and 1568  $\text{cm}^{-1}$  are red-shifted from the values for P3DTV at 1289, 1402, and 1582  $\text{cm}^{-1}$ , indicating more enhanced conjugation and thus reduced bandgap in P3DSV (vide infra). Expectedly, P3DSV-*co*-P3DTV shows peaks at 1284, 1400, and 1576  $\text{cm}^{-1}$ , between those of corresponding homopolymers, respectively. On the other hand, the blend displays Raman profiles as an overlap of those of the homopolymers, which is most clearly seen as the vinyl C=C stretch appears as two peaks at 1572 and 1582  $\text{cm}^{-1}$ . In the IR spectra (Figure S4B), several modes, at 792, 1011, 1086, and 1258  $\text{cm}^{-1}$  that most likely originate from C–H deformations of the selenophene ring,<sup>40,41</sup> are strongly enhanced in P3DSV while depressed in P3DTV. Similarly, the blend shows a spectrum as superposition from those of the homopolymers. P3DSV-*co*-P3DTV, however, displays a spectrum more resembling that of P3DSV with depression of peaks at about 550 and 1460  $\text{cm}^{-1}$  that are both present for the homopolymers.

Differential scanning calorimetry (DSC) experiments were performed on these polymers and blends, and the results are summarized in Figure S5. P3DSV and P3DTV show similar melting points at about 140 °C but different crystallization temperature at about 120 and 100 °C, respectively, indicating crystalline nature of these two polymers. The equal weight blend of P3DSV and P3DTV expectedly shows DSC traces that are superposition of those of corresponding homopolymers. However, both melting and crystallization events are suppressed for P3DSV-*co*-P3DTV, suggesting amorphous nature of the copolymer.

The impact on polymer electronic properties through Se substitution is first studied by UV–vis absorption spectroscopy. In dilute solutions (Figure 2A), both P3DTV and P3DSV display very similar structured absorption profiles, indicating collapsed conformation. Compared with P3DTV that has  $\lambda_{\text{max}}$  of 584 nm and absorption onset at 670 nm,  $\lambda_{\text{max}}$  and onset of P3DSV are red-shifted to 617 and 721 nm, respectively, confirming the bandgap reducing effect of Se incorporation (ca. 1.85 eV for P3DTV and 1.72 eV for P3DSV). On the other hand, P3DSV-*co*-P3DTV has an only slightly structured absorption profile with  $\lambda_{\text{max}}$  of 597 nm and onset at 700 nm, corresponding to a bandgap of about 1.77 eV. Both numbers

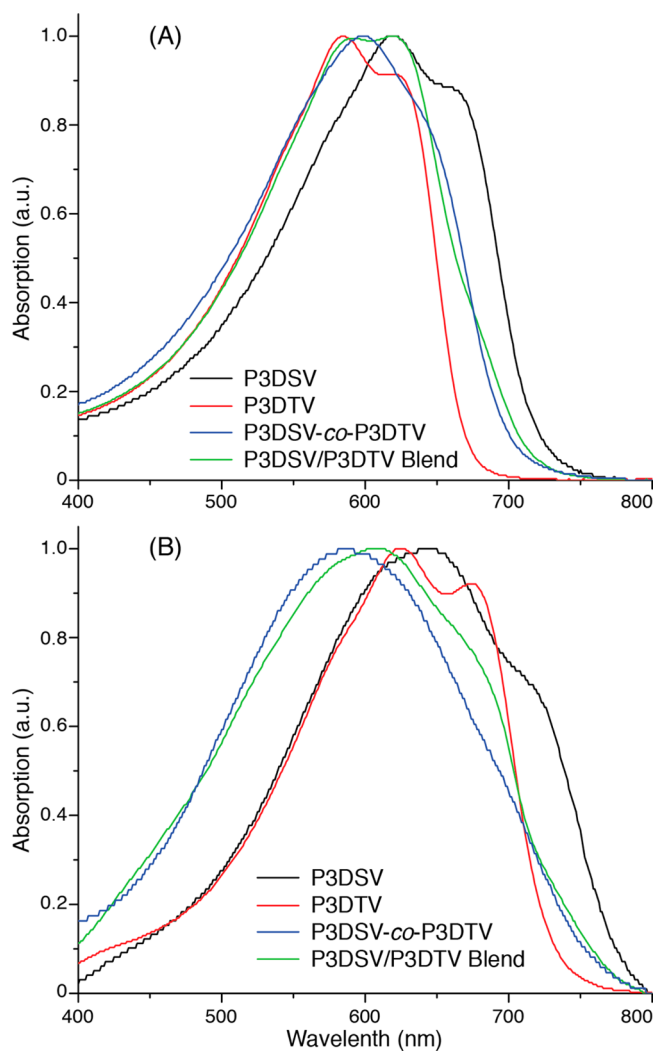


**Figure 2.** UV–vis absorption spectra of P3DSV (black), P3DTV (red), P3DSV-*co*-P3DTV (blue) and P3DSV/P3DTV blends (50/50, wt/wt, green): (A) in chlorobenzene solutions (ca.  $10^{-5}$  M r.p. units) and (B) as thin films spin-cast from chlorobenzene solutions onto glass substrates.

are in between those of the P3DTV and P3DSV homopolymers, suggesting an averaging effect on electronic properties through copolymerization. Such effect is further confirmed by the absorption profile of the simple blend solution of the two homopolymers, which display two identical  $\lambda_{\text{max}}$ s with those of P3DSV and P3DTV. Cyclic voltammetry (CV) was also performed on solutions of the polymers to estimate the energy levels as shown in Figure S6 and summarized in Table 1. Quasi-to nonreversible redox behaviors are observed for all three polymers tested, from the onsets of which the highest occupied

**Table 1. Electronic Properties of Polymers<sup>a</sup>**

	HOMO <sup>b</sup>	LUMO <sup>c</sup>	BG <sub>CV</sub> <sup>d</sup>	BG <sub>opt</sub> <sup>e</sup>
P3DSV	−4.62	−3.05	1.57	1.72
P3DTV	−4.73	−2.92	1.81	1.85
P3DSV- <i>co</i> -P3DTV	−4.75	−3.03	1.72	1.77

<sup>a</sup>All units in electronvolt (eV). <sup>b</sup>Highest occupied molecular orbital. <sup>c</sup>Lowest unoccupied molecular orbital. <sup>d</sup>Bandgap by cyclic voltammetry. <sup>e</sup>Optical bandgap in solution.



molecular orbital (HOMO) and lowest unoccupied molecular orbital (LUMO) energy levels are calculated. Interestingly, P3DSV-co-P3DTV has a HOMO level similar to that of P3DTV and a LUMO level close to that of P3DSV. Bandgap of the copolymer is in between those of the homopolymers, consistent with optical observations.

Very different trends are observed for the thin films of these polymers, as shown in Figure 2B. The absorption profiles of P3DTV and P3DSV are very similar to those reported earlier,<sup>21,32</sup> giving bandgaps of about 1.70 and 1.60 eV, respectively. The vibronic structures of P3DSV are less pronounced than those of P3DTV, indicating less efficient packing of P3DSV chains, presumably caused by the larger sizes of Se atoms. Surprisingly, the blend no longer shows superposition from the two homopolymers, and instead, only a weakly structured absorption profile with a  $\lambda_{\text{max}}$  at 607 nm is observed. P3DSV-co-P3DTV, on the other hand, shows an even more blue-shifted  $\lambda_{\text{max}}$  at 585 nm and an almost structureless profile. Both the blend and the copolymer have similar absorption onset at about 760 nm, corresponding to bandgaps of about 1.63 eV. These observations suggest that both the blend and the copolymer are disordered in the thin-film state.

In order to study the polymer packing structures in detail, powder X-ray diffraction (XRD) experiments were performed and the results are shown in Figure S7. All three polymers displayed three lamellar (X00) scattering peaks at  $2\theta$  values of about  $5.4^\circ$  for the (100) peak, corresponding to a  $d$ -spacing of about 16.3 Å that is consistent with previous reports and expected since these polymers all have similar structures and the same  $n$ -decyl side chains.<sup>21</sup> The peaks of P3DSV and P3DSV-co-P3DTV are apparently weaker and broader than those of P3DTV, proving the less crystalline nature of the Se containing polymers. Furthermore, weak scattering peaks are observed at  $2\theta$  values of  $21.3^\circ$  for P3DTV and  $20.7^\circ$  for P3DSV and P3DSV-co-P3DTV, corresponding to  $d$ -spacings of 4.16 and 4.29 Å, respectively. Based on previous reports,<sup>23,25</sup> we tentatively assign these peaks from  $\pi$ - $\pi$  stacking of the polymer main-chains. The slightly larger  $\pi$ - $\pi$  stacking distance observed in Se containing polymers is possibly caused by the larger sizes of Se atoms than those of S atoms, which induces less efficient packing of polymer chains and likely explains the reduced crystallinity in P3DSV and P3DSV-co-P3DTV.

In summary, we have successfully prepared two Se analogs of PTV through ADMET techniques. Physical and electronic properties of the resulting polymers can be tuned by the extents of replacement of S atoms with Se. We are currently studying the excited state dynamics in these P3DSV and copolymers, as well as their applications in optoelectronic applications.

## ■ ASSOCIATED CONTENT

### Supporting Information

Experimental details, GC-MS spectrum, kinetic plots, Raman/IR spectra, DSC traces, cyclic voltammograms, X-ray diffraction profiles, and NMR spectra. The Supporting Information is available free of charge on the ACS Publications website at DOI: 10.1021/acsmacrolett.5b00292.

## ■ AUTHOR INFORMATION

### Corresponding Author

\*E-mail: yangqin@unm.edu.

### Notes

The authors declare no competing financial interest.

## ■ ACKNOWLEDGMENTS

The authors would like to acknowledge University of New Mexico for financial support for this research. National Science Foundation (NSF) is acknowledged for supporting the NMR facility at UNM through grants CHE-0840523 and 0946690. The authors also thank Prof. Ramesh Giri (UNM) for helping acquire the GC-MS spectra.

## ■ REFERENCES

- (1) *Handbook of Conducting Polymers*, 3rd ed.; Skotheim, T. A.; Reynolds, J. R., Eds.; CRC Press: Boca Raton, FL, 2007.
- (2) Roncali, J. *Chem. Rev.* **1997**, *97*, 173–205.
- (3) Cheng, Y.-J.; Yang, S.-H.; Hsu, C.-S. *Chem. Rev.* **2009**, *109*, 5868–5923.
- (4) Boudreault, P.-L. T.; Najari, A.; Leclerc, M. *Chem. Mater.* **2011**, *23*, 456–469.
- (5) Huitema, H. E. A.; Gelinck, G. H.; van der Putten, J. B. P. H.; Kuijk, K. E.; Hart, C. M.; Cantatore, E.; Herwig, P. T.; van Breemen, A. J. J. M.; de Leeuw, D. M. *Nature* **2001**, *414*, 599.
- (6) Musser, A. J.; Al-Hashimi, M.; Maiuri, M.; Brida, D.; Heeney, M.; Cerullo, G.; Friend, R. H.; Clark, J. J. *Am. Chem. Soc.* **2013**, *135*, 12747–12754.
- (7) Jen, K.-Y.; Maxfield, M.; Shacklette, L. W.; Elsenbaumer, R. L. *J. Chem. Soc., Chem. Commun.* **1987**, 309–311.
- (8) Yamada, S.; Tokito, S.; Tsutsui, T.; Saito, S. *J. Chem. Soc., Chem. Commun.* **1987**, 1448–1449.
- (9) Gillissen, S.; Henckens, A.; Lutsen, L.; Vanderzande, D.; Gelan, J. *Synth. Met.* **2003**, *135–136*, 255–256.
- (10) Goldoni, F.; Janssen, R. A. J.; Meijer, E. W. *J. Polym. Sci., Part A: Polym. Chem.* **1999**, *37*, 4629–4639.
- (11) van de Wetering, K.; Brochon, C.; Ngov, C.; Hadziioannou, G. *Macromolecules* **2006**, *39*, 4289–4297.
- (12) Zhang, C.; Matos, T.; Li, R.; Sun, S.-S.; Lewis, J. E.; Zhang, J.; Jiang, X. *Polym. Chem.* **2010**, *1*, 663–669.
- (13) Toyoshima, R.; Akagi, K.; Shirakawa, H. *Synth. Met.* **1997**, *84*, 431–432.
- (14) Loewe, R. S.; McCullough, R. D. *Chem. Mater.* **2000**, *12*, 3214–3221.
- (15) Hou, J.; Tan, Z.; He, Y.; Yang, C.; Li, Y. *Macromolecules* **2006**, *39*, 4657–4662.
- (16) Delgado, P. A.; Liu, D. Y.; Kean, Z.; Wagener, K. B. *Macromolecules* **2011**, *44*, 9529–9532.
- (17) Qin, Y.; Hillmyer, M. A. *Macromolecules* **2009**, *42*, 6429–6432.
- (18) Speros, J. C.; Paulsen, B. D.; Slowinski, B. S.; Frisbie, C. D.; Hillmyer, M. A. *ACS Macro Lett.* **2012**, *1*, 986–990.
- (19) Speros, J. C.; Paulsen, B. D.; White, S. P.; Wu, Y.; Jackson, E. A.; Slowinski, B. S.; Frisbie, C. D.; Hillmyer, M. A. *Macromolecules* **2012**, *45*, 2190–2199.
- (20) Speros, J. C.; Martinez, H.; Paulsen, B. D.; White, S. P.; Bonifas, A. D.; Goff, P. C.; Frisbie, C. D.; Hillmyer, M. A. *Macromolecules* **2013**, *46*, 5184–5194.
- (21) Yang, G.; Hu, K.; Qin, Y. *J. Polym. Sci., Part A: Polym. Chem.* **2014**, *52*, 591–595.
- (22) Smith, A. P.; Smith, R. R.; Taylor, B. E.; Durstock, M. F. *Chem. Mater.* **2004**, *16*, 4687–4692.
- (23) Kim, J. Y.; Qin, Y.; Stevens, D. M.; Ugurlu, O.; Kalihari, V.; Hillmyer, M. A.; Frisbie, C. D. *J. Phys. Chem. C* **2009**, *113*, 10790–10797.
- (24) Stevens, D. M.; Qin, Y.; Hillmyer, M. A.; Frisbie, C. D. *J. Phys. Chem. C* **2009**, *113*, 11408–11415.
- (25) Gao, J.; Thomas, A. K.; Yang, J.; Aldaz, C.; Yang, G.; Qin, Y.; Grey, J. K. *J. Phys. Chem. C* **2015**, *119*, 8980–8990.
- (26) Olejnik, E.; Pandit, B.; Basel, T.; Lafalce, E.; Sheng, C.-X.; Zhang, C.; Jiang, X.; Vardeny, Z. V. *Phys. Rev. B* **2012**, *85*, 235201.
- (27) Zade, S. S.; Zamoshchik, N.; Bendikov, M. *Chem.—Eur. J.* **2009**, *15*, 8613–8624.
- (28) Patra, A.; Bendikov, M. *J. Mater. Chem.* **2010**, *20*, 422–433.

(29) Hollinger, J.; Gao, D.; Seferos, D. S. *Isr. J. Chem.* **2014**, *54*, 440–453.

(30) Heeney, M.; Zhang, W.; Crouch, D. J.; Chabinyk, M. L.; Gordeyev, S.; Hamilton, R.; Higgins, S. J.; McCulloch, I.; Skabara, P. J.; Sparrowe, D.; Tierney, S. *Chem. Commun.* **2007**, 5061–5063.

(31) Ballantyne, A. M.; Chen, L.; Nelson, J.; Bradley, D. D. C.; Astuti, Y.; Maurano, A.; Shuttle, C. G.; Durrant, J. R.; Heeney, M.; Duffy, W.; McCulloch, I. *Adv. Mater.* **2007**, *19*, 4544–4547.

(32) Al-Hashimi, M.; Baklar, M. A.; Colleaux, F.; Watkins, S. E.; Anthopoulos, T. D.; Stingelin, N.; Heeney, M. *Macromolecules* **2011**, *44*, 5194–5199.

(33) Bedi, A.; P, S. S.; Narayan, K. S.; Zade, S. S. *Macromolecules* **2013**, *46*, 5943–5950.

(34) Lehmann, C. W.; Wagener, K. B. In *Handbook of Metathesis*; Grubbs, R. H., Ed.; Wiley-VCH Verlag GmbH&Co: Weinheim, 2003; Vol. 3.

(35) Opper, K. L.; Wagener, K. B. *J. Polym. Sci., Part A: Polym. Chem.* **2011**, *49*, 821–831.

(36) Mutlu, H.; de Espinosa, L. M.; Meier, M. A. R. *Chem. Soc. Rev.* **2011**, *40*, 1404–1445.

(37) Hollinger, J.; Jahnke, A. A.; Coombs, N.; Seferos, D. S. *J. Am. Chem. Soc.* **2010**, *132*, 8546–8547.

(38) The relative intensities of the GC peaks are different than those obtained from  $^1\text{H}$  NMR integration. We suspect that this difference is due to double bond thermal isomerization, most likely from *cis* to *trans*, within the GC column. We have observed similar transformations in *cis*-3DTV as previously reported by us (ref 21).

(39) Maity, P.; Kundu, D.; Roy, R.; Ranu, B. C. *Org. Lett.* **2014**, *16*, 4122–4125.

(40) Gerding, H.; Milazzo, G.; Rossmark, H. H. K. *Recl. Trav. Chim. Pays-Bas* **1953**, *72*, 957–962.

(41) Poletti, A.; Cataliotti, R.; Paliani, G. *Chem. Phys.* **1974**, *5*, 291–297.